



## Autoclave-assisted Green Synthesis of Gumkaraya-based Silver nanoparticles and its Antibacterial Potentials

Shyamala Chandra Rakkala, Vidya Chernapalli, Suresh Velpula and Karuna Rupula\*

Department of Biochemistry, University College of Science,  
Osmania University, Hyderabad (Telangana), India.

(Corresponding author: Karuna Rupula\*)

(Received: 16 January 2023; Revised: 13 February 2023; Accepted: 20 February 2023; Published: 22 March 2023)

(Published by Research Trend)

**ABSTRACT:** The rise of multidrug-resistant bacterial strains and the lack of therapeutically effective treatments have enhanced the need for the development of innovative antibacterial agents more evident in recent years. Due to their proven antibacterial activity, silver nanoparticles (AgNPs) are of great interest in treating bacterial infections. Highly stable silver nanoparticles have been synthesized using solubilized karaya gum (KG) by autoclave method. The stability of karaya-based nanoparticles (KG-AgNPs) influenced by various factors such as reaction time, pH, ionic and gum concentrations were investigated. The synthesized silver nanoparticles were characterized by UV-Vis spectroscopy, FTIR, XRD, SEM, and TEM. The synthesized KGAgNPs showed significant antibacterial activity on both the gram-positive (*S. aureus*) and gram-negative (*P. aeruginosa*) bacteria with a zone of inhibition 13 and 15 mm respectively. The minimum inhibitory concentration (MIC) of the KG-AgNPs for *S. aureus* and *P. aeruginosa* were determined as 14 and 10 µg/mL, respectively. The mode of action studies were based on analysis of (membrane damage, K<sup>+</sup> ion leakage, and status of ROS) which revealed that the KG-AgNPs act as efficient antibacterial agents. In the present study AgNPs were synthesized using a natural biopolymer (KG) directly without the role of any reducing agent and the as synthesized nanoparticles act as a potent antibacterial agents for pharmaceutical applications in near future. In conclusion, the KG-AgNPs synthesized were highly stable and effective antibacterial agents.

**Keywords:** Silver nanoparticles, Green synthesis, Karaya gum, antibacterial activity, oxidative stress, mode of action.

### INTRODUCTION

Materials in the size range of 1-100 nm dimensions are considered nanomaterials. Nanoscale materials have emerged as an exciting class of materials for their high demand in the fields of electronics, pharmaceutical, cosmetics, medical, fertilizer, petrochemicals, textile industry, and environmental sectors (Costa and Rossi, 2012). Among all nanomaterials, metal nanoparticles are gaining considerable importance due to their promising applications in several areas of research. Particularly the noble metals including silver, gold, and platinum are finding potential applications in biological systems due to their transient nature and nontoxic properties (Subbaiah and Beedu 2018; Venkatesham *et al.*, 2014). At present, the researchers are focusing more on eco-friendly, green synthesis approaches for the efficient synthesis of commercially important metal nanoparticles (Dauthal and Mukhopadhyay 2016; Velpula *et al.*, 2022). Nanotechnology offers enormous potential in healthcare, notably for the production of improved medications (Seema *et al.*, 2016).

A facile, eco-friendly green chemistry-based synthesis of silver nanoparticles was performed using Karaya

gum which is alternatively known as Indian tragacanth and obtained as a dried exudate from the tree *Sterculia urens*. The karaya gum (KG) is an acidic polysaccharide composed of galacturonic acid, β-D-galactose, glucuronic acid, L-rhamnose, and other residues. The gum is non-toxic and well-known for unique features such as acid and heat stability, high viscosity, high swelling and water retention capacity, bioavailability, and high resistance to antimicrobial activity (Anderson and Stoddart 1966).

With the revolutionary discovery of the major groups of antibiotics (tetracyclines, cephalosporins, aminoglycosides, and macrolides) in the “golden era” the main problem of chemotherapy was solved in the 1960s. The increasing resistance to antibiotics by pathogenic bacteria and fungi nowadays is posing a serious problem to the society. These antibiotics are in danger of losing their efficacy due to increased microbial resistance (Mayers *et al.*, 2009). In the present situation, its impact on treatment failure is considerably associated with pathogenic bacteria that are multi-drug-resistant and has become a global concern in society (Guschin *et al.*, 2015; Martin *et al.*, 2015). In this situation, a green synthesis-based nano silver is an ideal and excellent choice (Srikar *et al.*,

2016). The use of silver nanoparticles in the surface sterilization of seeds to aid in enhanced seed germination was reported by Kumari *et al.* (2021). The percentage of germination in seeds and seedling growth is improved by seed nano priming (Dutta *et al.*, 2021). For this reason, researchers worldwide are working and trying to produce new, commercial, and effective antimicrobial agents even against resistant bacteria (Gelatti *et al.*, 2009; Rastogi *et al.*, 2015). There are several instances of widespread use of silver since prehistoric times as an efficient anti-microbial agent (Rai *et al.*, 2009). Silver nanoparticles have wide research-based and technological applications because of their ease in eco-friendly green synthesis and synthetic stability, which led to their recognition as efficient and outstanding antimicrobial agents (Jaiswal *et al.*, 2010; Kora and Sashidhar 2015).

In the current study, our attempt was to develop a facile and eco-friendly potential antibacterial agent in the form of silver nanoparticles by using solubilized karaya gum and its characterization. Optimized reaction conditions resulted in monodisperse, spherical, and size-controlled silver nanoparticles. The antimicrobial, as well as the mode of action of KG-AgNPs on the bacterial cell membrane, was studied on *S. aureus* and *P. aeruginosa* employing basic antibacterial assays. Analysis of morphological changes through scanning electron microscopy (SEM), the status of reactive oxygen species (oxidative stress), and impact on membrane integrity and permeability were also carried out.

## MATERIALS AND METHODS

**Chemicals.** Silver Nitrate ( $\text{AgNO}_3$ ) was purchased from Sigma-Aldrich (St Louis, USA). Gum Karaya (KG) grade 1 was procured from Girijan Cooperative Corporation, Hyderabad, Government of Telangana, India. All the other chemicals and reagents used for the study are of analytical grade and are freshly prepared before the analysis.

### Methods

**Synthesis of gum karaya-based biocomposite silver nanoparticles.** The gum exudate was powdered in a mechanical blender (Philips, Mumbai, India) at high speed, and then the powder was sieved using a test sieve of (45  $\mu\text{m}$  mesh size). Later 2.0 g of accurately weighed gum powder was dispensed into 100 mL of Milli Q water (18.2  $\text{M}\Omega\cdot\text{cm}$ ) taken in a fresh plastic beaker and gently stirred overnight at room temperature (37°C) on a magnetic stirrer (2000 rpm) to obtain whole gum (2%) solution, which was followed by centrifugation at 5000 rpm for 10 minutes. Then the solution was centrifuged to collect the soluble gum from the supernatant and freeze-dried. The dried powder was used for the preparation of nanocomposites. From the stock solution (10 mM) of silver nitrate ( $\text{AgNO}_3$ ) required volume was taken and added to varying concentrations of soluble gum karaya solution (0.2-1.0%) to get a final concentration of 1 mM of  $\text{AgNO}_3$ . 0.1M HCl and 0.1M NaOH are used to adjust the pH of the KG- nanoparticle solutions. The gum and  $\text{AgNO}_3$  solutions were then autoclaved at 121

°C and 15 psi for 30 minutes in a semi-automatic autoclave (Ketan SA-35) for the formation of nanoparticles. Various concentrations of gum (0.2-1.0%), and different pH conditions (4, 5, 6, 7, and 8) were also assessed. The nanoparticles formed exhibited a colour change a preliminary observation which was followed by UV-vis spectrophotometric analysis (Vinod and Sashidhar 2011; Velpula *et al.*, 2021; Kalaignana *et al.*, 2017).

### Characterization of Karaya Gum-based silver nanocomposites

**UV-visible Spectrophotometric analysis.** UV-vis spectrophotometer (Agilent Cary 60 UV-VIS Spectrophotometer, Agilent Technologies, California, USA) with a spectral resolution of 1 nm from 200 to 800 nm was used to analyze the formation of silver nanoparticles. The distinctive absorbance of KG-nanocomposite solutions was recorded. The absorption spectrum of the native gum solution before and after autoclaving was also measured taking deionized water (Milli Q) as blank. The KG-AgNPs synthesized were stored in cold (4°C) and evaluated for their stability at different time periods (0,90 and 180 days) also.

**Fourier transform infrared spectroscopy (FT-IR) analysis.** A Fourier transform infrared spectrophotometer (FTIR-8400S, Shimadzu, Tokyo, Japan), over a spectral range of 4000–400  $\text{cm}^{-1}$  and resolutions at 4  $\text{cm}^{-1}$  was used to record the FT-IR spectra of the KG-based nanocomposites. Both the spectra of native soluble gum KG (1%) and KG-nanocomposites were recorded to identify the functional groups involved in reducing and capping the nanoparticles.

**Scanning electron microscopy coupled Energy Dispersive X-ray (SEM-EDXA) analysis.** The native gum (solubilized) and KG-nanocomposites were analyzed using a scanning electron microscope (ZEISS Gemini SEM, Denmark) coupled with INCAx-act Oxford Instruments Energy Dispersive X-ray analysis (High Wycombe, UK) (SEM-EDX) to examine their surface morphology. The freeze-dried KG-AgNPs were mounted on a stainless-steel stab with a thin layer of gold-coated double-sticktape. The samples were examined under high vacuum conditions. The Tungsten filament solution was fixed at 3.5 nm, 2.5 nm for LaB6 filament, and 133 eV. for the EDX detector.

**Transmission electron microscopy (TEM) analysis.** A transmission Electron Microscope (TEM) was used for measuring the size and shape of the KG-AgNPs (Model FEI Tecnai G2S- TWIN, Czech Republic). The KG-AgNPs (sample 10-20  $\mu\text{L}$ ) was applied on a carbon-coated copper grid and allowed to dry at 37 °C and then examined by TEM. Gatan software provided by the manufacturer was used to record the micrographs of KG nanocomposites.

**X-ray diffraction (XRD) analysis.** The physical nature of the KG-AgNPs synthesized and the native gum (solubilized) were analyzed using a diffractometer (Bruker XRD D8 Advance, Germany) equipped with a graphite monochromatic Cu-K $\alpha$  radiation ( $\lambda = 1.5406 \text{ \AA}$ ). The samples were processed into a fine powder and placed in the instrument. Measurements were made by

a step-scanning program (0.02° per step) with acquisition time (5s per step). The Diffractograms were run in the range of 3.5–70° with a scanning speed of 2° min<sup>-1</sup> and chart speed of 2°/2 cm per 2θ. The data obtained were processed using in X'Pert High Score software provided with the instrument.

**Inductively coupled plasma–mass spectrometry (ICP-MS) analysis.** ICP-MS was employed to find the concentration of Ag in the ionic solution and the synthesized KG-AgNPs were determined by subjecting to acid digestion by adding aliquots (0.005 mL, equivalent to 0.005 g) of the nanocomposite solutions to nitric acid (1mL; 69% [v/v]) and incubating overnight. The volume of the digested samples was then made up to 10 mL with deionized water (Milli Q) and the digested samples and the reference standards were then analyzed by ICP-MS. The Quantification of the nano-metal concentrations in the GK-nanocomposite preparations was done using the ICP-MS metal analyzer 7700X instrument (Agilent Technologies, Inc., Santa Clara, CA, USA). Prior to the operation, the purging of the instrument was done using auxiliary gas (1.0 L min<sup>-1</sup>), plasma gas (15 L min<sup>-1</sup>), and carrier gas (1.0 L min<sup>-1</sup>). The pressure of the argon gas cylinder was maintained in the range of 650–720 kPa. The values thus obtained were evaluated using the Mass Hunter software.

**Particle size and zeta potential analysis.** The size and charge of KG-AgNPs were also analyzed using Delsa Max PRO (Beckman Coulter, Inc., Brea, CA, USA). Based on dynamic light scattering pattern, the size distributions were analyzed with 10 numbers of acquisitions for 2sec. Phase-analyzed light scattering (PALS) based analysis of the zeta potentials of nanomaterials was obtained with the electric field frequency of 10Hz, amplitude voltage of 3volts, laser mode of 45 mV, and collection period of 20s. Both the size and zeta potentials of particles were optimized with the calibration standards before performing analysis and all the experiments were carried out at 25 °C. The size and zeta potential of native gum (solubilized) was also analyzed for comparison.

#### **Antibacterial assays of the KG-based silver nanoparticles**

**Well diffusion assay.** Two bacterial strains *S. aureus* (ATCC 25923) gram-positive, and *P. aeruginosa* (ATCC 27853) gram-negative were selected to study the antibacterial activity of Karayagum-based bio-composite silver nanoparticles as described by Kora *et al.* (2010). The bacterial cultures kept on sheep blood agar medium slants with periodic sub-culturing every 15 days of interval period were used for the study. The bacterial suspension was prepared by picking up a single colony from the culture slants and grown overnight in Lysogeny Broth (LB) medium and then the turbidity was adjusted to 0.5 Mc Farland standard. The adjusted cultures were then diluted with Mueller Hinton Broth (MHA) to obtain the bacterial suspension of approximately 10<sup>5</sup> CFU mL<sup>-1</sup>. Mueller Hinton agar (MHA) plates were inoculated with these bacterial cultures and different concentrations of KG-AgNPs (8-50µg/mL) were added to the well with a diameter of 6

mm. Autoclaved gum karaya (1%) and antibiotic amikacin (0.5-1.0µg/mL) were used as negative and positive controls. The plates were incubated at 37°C for 24 h in a bacteriological incubator and the zone of inhibition (ZOI) was calculated by deducting the well diameter from the total inhibition zone diameter (Kora *et al.*, 2010).

**Micro-broth dilution method.** The minimum inhibitory concentration (MIC) of KG -AgNPs against the test bacterial strains was determined by the micro-broth dilution method as described by Muchintala *et al.* (2020). The sterile polystyrene microtiter plate wells were loaded with different concentrations of KG-AgNPs (1-20 µg /mL) and 200µLof nutrient broth containing 10<sup>6</sup> CFU/mL of inoculum. These plates were incubated at 37°C for 48 h in static condition. The control wells were also maintained with a medium containing bacterial suspension. The MIC values were determined by measuring the visual turbidity developed in the wells and the absorbance at 600 nm, using a microtiter plate (ELISA) reader (Micro Scan, MS5608A, ECIL, India). The lowest concentration at which there was no increase in absorbance was considered as MIC.

#### **Mechanism of action of KG-AgNPs**

**Measurement of Cytoplasmic contents of the bacterial cell.** Cytoplasmic leakage analysis of the bacterial strains treated with the KG-AgNPs was evaluated based on a standard protocol with few modifications (Kora and Sashidhar 2015; Muchintala *et al.*, 2020). To further know the effect of KG-AgNPs on membrane damage, nucleic acids and proteins leaked from the bacterial cell membrane were measured using a UV-vis spectrophotometer (Agilent Cary 60 UV-VIS Spectrophotometer, Agilent Technologies, California, USA). The bacterial cell suspension was prepared in sterile saline with an absorbance of 0.5 at 600 nm and treated with (8-15 µg/mL) of KG-AgNPs for 1 hour. The culture sample without the nanoparticles was treated as negative control and the culture sample subjected to 30 min of heating in a boiling water bath was considered as positive control. The samples were centrifuged for 15 min at 10,000 rpm and the supernatant absorbance was recorded at 260 and 280 nm.

**Measurement of Intracellular potassium (K+) ion leakage.** Analysis of potassium (K+) leakage was analyzed in the bacterial suspensions treated with KG-AgNPsto test their effect on the bacterial membrane (Rastogi *et al.*, 2015). The bacterial cells grown to the exponential phase were treated with KG-AgNPs at their MIC concentration and kept for incubation for 1 h at 37°C positive and negative controls were also maintained as culture samples with 70% ethanol-treated cells (50 µL/mL) and culture samples without any KG-AgNPs respectively. Then the cells were subjected to centrifugation at 5000 rpm for 10 min. The supernatants collected were analyzed for potassium ion content by inductively coupled plasma mass spectroscopy (ICP-MS) metal analyzer 7700 × instrument (Agilent Technologies, Inc., Santa Clara, CA, USA).

**Measurement of intracellular reactive oxygen species (ROS).** The detection of intracellular reactive oxygen species (ROS) (Kora and Sashidhar 2015) in KG-AgNPs treated bacterial cells was estimated by using dichloro-dihydro-fluoresce in diacetate (H<sub>2</sub>DCFDA) fluorescent dye, a common ROS indicator. Stock solution of H<sub>2</sub>DCFDA (2mM) prepared in dimethyl sulfoxide (DMSO) and stored at -40°C in dark. Bacterial cultures were harvested, washed, and resuspended in 0.1 M Sodium Phosphate buffer, pH 7.2, which were grown in nutrient broth overnight, and then the cell suspension was adjusted to obtain an A<sub>600nm</sub> of 0.5. To this bacterial suspension of 20 ml, 2 mM H<sub>2</sub>DCFDA(100 µl stock solution was added to get a final concentration of 10µM)and incubated in dark at 37°C for 60 min. The cells were washed and resuspended in 0.1 M Sodium Phosphate Buffer. Then aliquots of the cell suspension were dispensed (200 µL) into 96 well-black Corning Costarmicrotitre plate (New York, USA) to which the KG-NPs (2 µg /mL) were added and incubated under dark at 37 °C for 60 min. The positive and negative controls were maintained with 30 µM H<sub>2</sub>O<sub>2</sub> treated bacterial suspensions and KG-AgNPs free respectively. At the end of 60 min, the fluorescence intensity was recorded with a Biotek Synergy™ H1 plate reader (Winooski, USA) at an emission wavelength of 520 nm and an excitation wavelength of 490 nm.

#### Scanning Electron Microscopy Studies

The morphological changes of bacterial cells (*S. aureus* and *P. aeruginosa*) before and after treatment with synthesized nanoparticles (GK-AgNPs) were captured with Scanning electron microscopy. Bacterial fixation studies were performed with few modifications (Rastogi *et al.*, 2015). A single colony picked from the bacterial culture was grown to the exponential phase and this actively grown culture was centrifuged at 10,000 g for 10 min. The cells were then washed thrice with 0.1 M PBS (pH 7.4) for 15 min each and fixed in 2.5% (v/v) glutaraldehyde at 4°C for 12 h. Then, the bacteria were washed three times with PBS (pH 7.4) and a series of graded ethanol (25%, 50%, 75%, and 100%) is used to dehydrate the cells for 15 min each. Then the specimens were observed using a scanning electron microscope (ZEISS Gemini SEM, Denmark) upon freeze-drying and gold coating of the specimens. The samples without the nanoparticles served as negative controls whereas heat-treated cells in a boiling water bath for 30 min were used as positive control.

**Statistical analyses.** The data recorded in the experimental analysis was statistically analyzed using Graph-Pad Prism and Origin Pro 7.0 software. The values reported are mean ± SD.

## RESULTS AND DISCUSSION

**Synthesis of gum karaya-based silver nanoparticles.** Silver in its nanoform exhibits a variety of properties and is known for its extensive applications in several fields (Srikar *et al.*, 2016; Mahapatra *et al.*, 2017; Natsuki *et al.*, 2015). The current study reports the green synthesis of silver nanoparticles using soluble gum karaya by autoclaving. The karaya gum-based silver nanoparticles were synthesized using solubilized gum at varying concentrations (0.2% to 1%) and AgNO<sub>3</sub> (0.5-5mM). The effect of pH on nanoparticle formation was also assessed. The prepared silver nanoparticles are first identified by a preliminary observation, based on the visual colour change of the solution. After autoclaving, the solution containing AgNO<sub>3</sub> and KG changed from light yellow to a deeper yellow colour which indicated the formation of KG-AgNPs. When subjected to autoclaving, the karaya gum biopolymer resulted in the reduction of metal ions from Ag<sup>+1</sup> to Ag<sup>0</sup> (Kora *et al.*, 2010). The nanoparticle formation was further analyzed by a UV-vis spectrophotometer.

**Effect of karaya gum concentration.** A vital role is played by gum concentration in nanoparticle synthesis (Velpula *et al.*, 2021). The results recorded depicted that GK-AgNPs exhibited specific absorbance at 430nm, while the native KG did not show any specific absorbance and the AgNO<sub>3</sub> depicted an absorbance at 280nm (Fig. 1A). With the increase of gum concentration from 0.2% – 1.0%, the absorbance values also increased. An optimal absorbance value was observed at a concentration of 1.0% percent gum. These results showed that the concentration of gum is directly proportional to the nanoparticle formation. Therefore, the nanoparticles for the study were prepared using 1% KG.

**Effect of ionic concentration of AgNO<sub>3</sub>.** Based on the above results 1 % gum was used for synthesis with varying concentrations of AgNO<sub>3</sub> (0.5-5 mM). The synthesis of nanoparticles is influenced by different ionic concentrations and an ionic concentration of 1 mM was found to be ideal for nanoparticle synthesis (Fig.1B). Hence all the nanoparticles were synthesized using 1% karaya gum and 1mM AgNO<sub>3</sub> solutions.

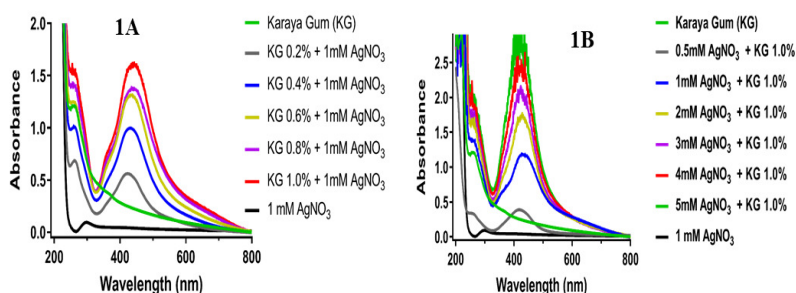


**Fig. 1 A.** Effect of gum karaya (KG) concentration (0.2-1.0 %); **B.** Effect of (AgNO<sub>3</sub>) concentration (0.5-5.0 mM) in the formation of GK-AgNPs.

**Effect of pH.** The synthesis of nanoparticle formation is influenced by different pH conditions. The absorbance of nanoparticles synthesized at different pH (3.0, 4.0, 5.0, 6.0, 7.0, and 8.0) was recorded against blank from 200 to 800nm as depicted in Fig. 2. Each

metal exhibits an optimal pH which is ideal for nanoparticle formation. A pH of 7.0 was determined to be optimal for KG-AgNPs synthesis. Based on these results the silver nanoparticles synthesis was performed within the pH range of 6-7.

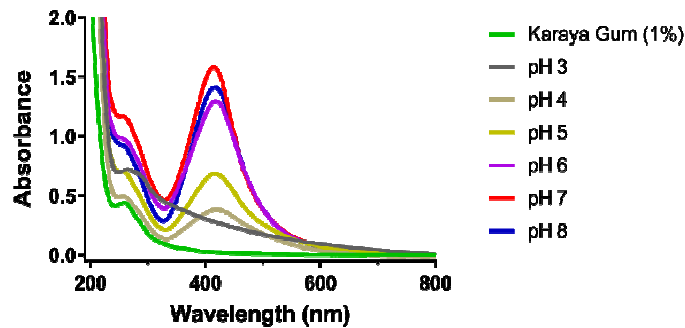


Fig. 2. Effect of pH on the formation of KG-AgNPs.

**Effect of time points on autoclaving.** The nanoparticles were synthesized with 1% karaya gum and 1mM AgNO<sub>3</sub> by autoclaving at different (15, 30, 45, 60min) time intervals (Fig. 3). The nanoparticles synthesized at 15 min and 30 min autoclaving time showed significant differences (higher absorbance at 30 min) in the absorbance recorded. However, the nanoparticles synthesized at 30min, 45min, and 60 min did not show any significant change in absorbance.

Therefore, autoclaving time duration of 30 min was found suitable for nanoparticle synthesis.

**Stability studies: Effect of time period.** The KG-AgNPs synthesized were stored in cold (4 °C) and evaluated for their stability. The UV-vis spectroscopic analysis was carried out and recorded at the end of the time period depicted (Fig. 4). The results indicated that the KG-AgNPs were highly stable for up to 180 days.

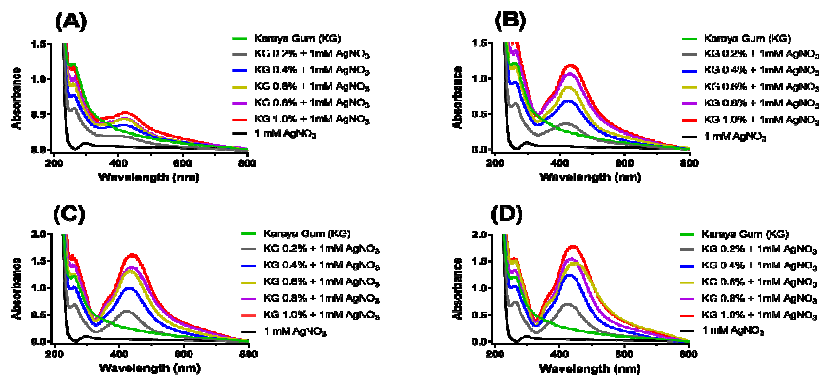


Fig. 3. UV-visible absorption spectra of KG-AgNPs synthesized at different time points. A. 15 min, B. 30 min, C. 45 min D. 60min of autoclaving.

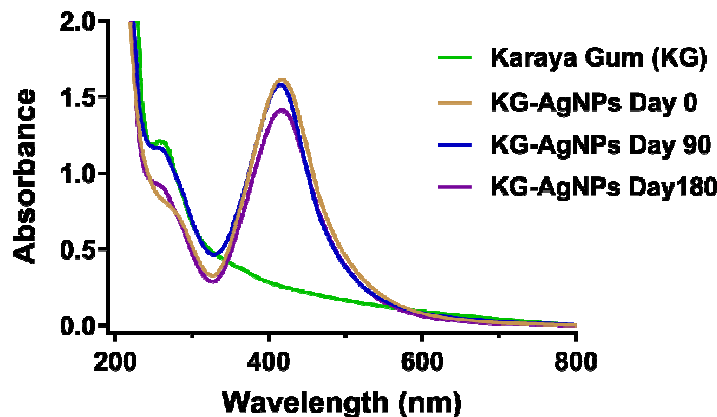


Fig. 4. Stability of synthesized nanoparticles (KG-AgNPs) assessed with various time points like 0, 90, and 180 days incubation at room temperature.

## Characterization of Gum karaya-based silver nanocomposites

**UV-vis spectrophotometric analysis.** The UV-visible spectral analysis was used to study the surface plasmon resonance (SPR) for silver nanoparticles as an indicator of preliminary confirmation for the synthesized nanoparticles. A periodic optical absorbance scan of the nanoparticles synthesized was recorded using a UV-vis

spectrophotometer. The characteristic SPR recorded in UV-vis absorption spectra (200-800nm) for the KG-Ag nanoparticles are represented in Fig. 5. The silver nanoparticles generated showed a distinctive peak at 430nm with 1% soluble karaya gum, 1mM AgNO<sub>3</sub>, pH 7, and 30min of autoclaving depicting its typical SPR, which was found to be optimal.

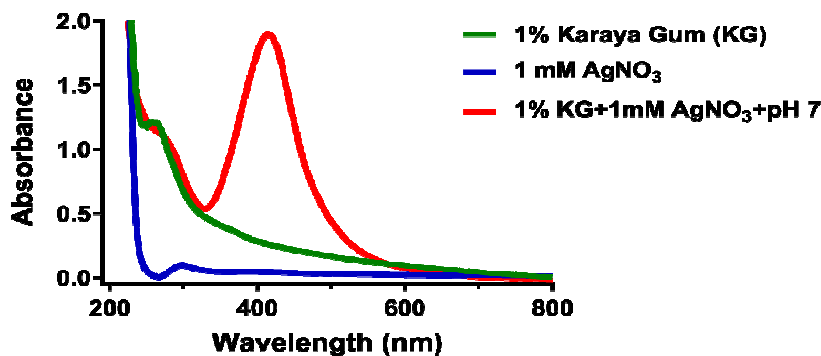


Fig. 5. Synthesis of nanoparticles (KG-AgNPs) after all the standardized conditions like gum concentration, ionic concentration, time, pH, and stability.

**Fourier transform infrared (FT-IR) spectroscopy analysis.** The FT-IR analysis revealed that redox reactions between the gum karaya backbone and the metal ions of Ag are due to the presence of various functional groups in the gum which were involved in the redox reactions (Fig. 6). The native gum and KG-AgNPs are compared to identify the altered intensities of the functional groups. The presence of (–OH), (CH<sub>3</sub>–CO–), and (–CH<sub>3</sub>CO) indicative of acetyl groups; (–COO–) and (–COO–) of carboxylate groups of uronic acid residues as major functional groups in the native KG was indicated by the spectra recorded at specific

wave numbers of 4702 cm<sup>-1</sup>, 1726 cm<sup>-1</sup>, 1525 cm<sup>-1</sup>, 1610 cm<sup>-1</sup>, and 1425 cm<sup>-1</sup> as depicted in Fig 6. The spectra of the functional groups were altered in the KG-based nanocomposites due to bond stretching and bending indicating the chemical interactions between the gum matrix and the nanocomposites formed. The FTIR spectra indicated the involvement of (–OH), (CH<sub>3</sub>–CO–), (–CH<sub>3</sub>CO) indicative of acetyl groups and (–COO–), (–COO–) of carboxylate groups of uronic acid residues as major functional in the reducing and capping of the AgNPs.

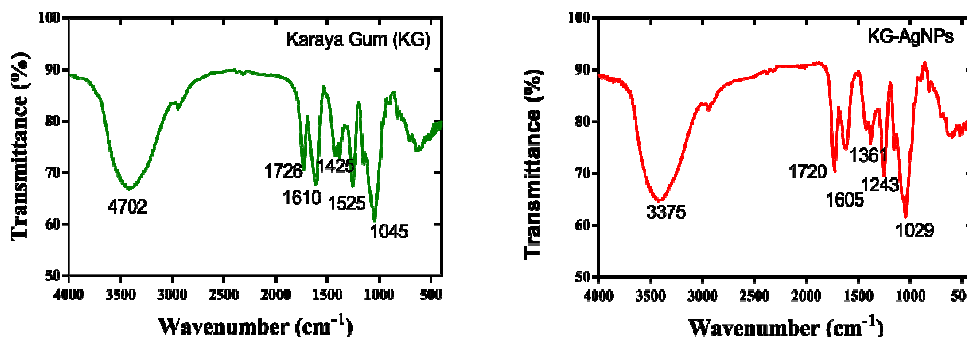
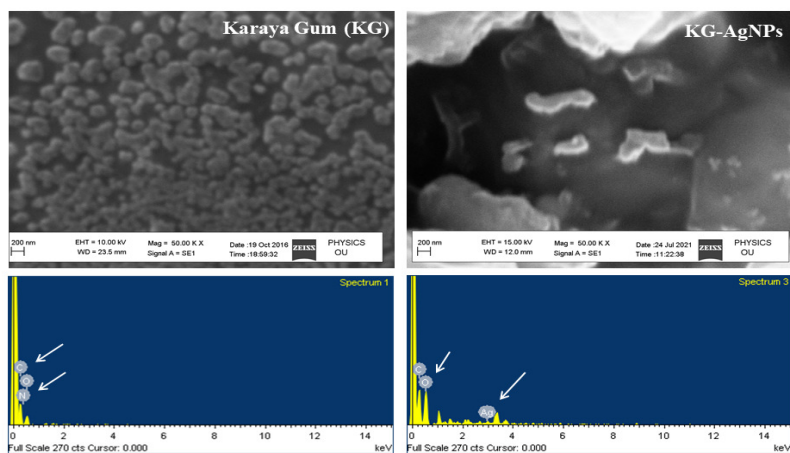


Fig. 6. The identification of functional groups presents on gum karaya and KG-AgNPs analyzed using FT-IR spectrum.

**SEM-EDX analysis.** The morphological structure and topographical features of the synthesized nanocomposites were revealed by SEM-EDX. The native gum sample analysis indicated its highly filamentous nature, while uniform distribution and nanoparticles in the bounded form on the gum matrix were observed in the KG-based nanocomposites. The SEM analysis was coupled to the EDXA which

revealed the elemental composition of the samples. The strong signals detected indicate the presence of metal atoms (Ag) in the densely populated nanoparticle regions while the weak signals indicate the presence of C, O, N, K, Cl, and Na atoms on the gum matrix recorded in the EDXA (Energy Dispersive Analysis of X-rays) (Fig. 7).



**Fig. 7.** SEM (scanning electron microscope) analysis of Gum karaya, KG-based silver nanoparticles and along with its EDX analysis

**Transmission electron microscopic analysis (TEM).** The KG-nanocomposites synthesized were analyzed by TEM to determine the size and their topographical features. The TEM images showed regularly dispersed, spherical nanostructures that were almost within the range of 12 to 20 nm in diameter and, were clearly embedded on the surface of the gum were noticed. Highly monodispersed nanoparticles with an average particle size of  $18.6 \pm 3.1$  nm within the gum matrix were observed for the KG-AgNPs (Fig. 8). These results confirm the efficient property of this gum in the synthesis of the AgNPs, as the size and shape of the

nanomaterials have been reported to influence their biological applications largely (Venkatesham *et al.*, 2014).

**X-ray diffraction analysis.** The soluble gum karaya and gum-based silver nanocomposites were characterized by XRD. Based on the characteristic diffract to gram pattern in the KG-AgNPs the signals recorded 111, 200, 220, and 311 corresponded to the presence of AgNPs. The XRD patterns of the nanocomposites revealed the crystalline nature of KG-AgNPs, while the native karaya gum was amorphous in nature (Fig. 9).

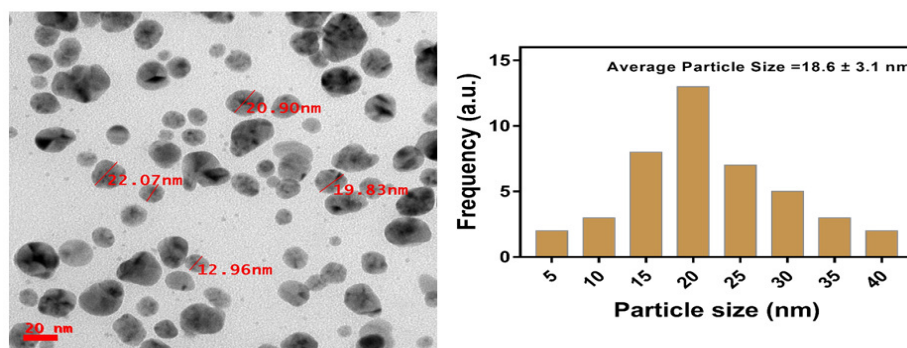


**Fig. 8.** TEM micrographs for gum karaya-based silver nanoparticles with corresponding histograms of particle size distributions.

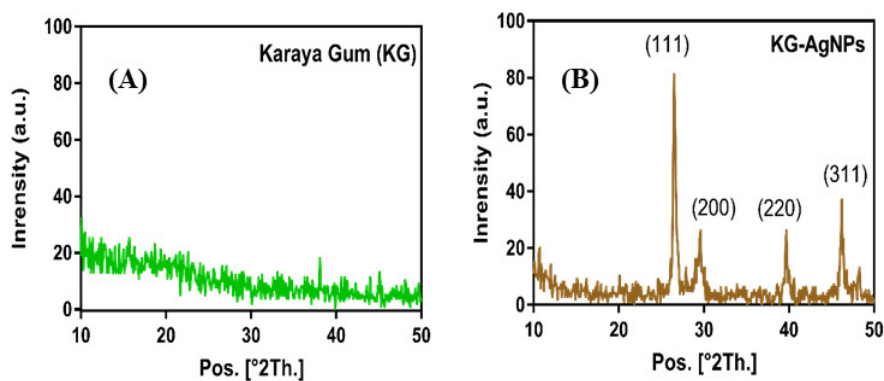


**Fig. 9.** X-Ray Diffraction (XRD) pattern of the gum and nanoparticles (A) Native karaya gum (KG), (B) KG-AgNPs.

**Particle size and zeta potential analysis.** The particle size (nm) and zeta potential (mV) for each of the KG-AgNPs synthesized, were determined using the nanoparticle analyzer based on dynamic light scattering (DLS) and phase-analysis light scattering (PALS). The experiment was carried out in triplicates to determine the particle size and zeta analysis for the synthesized nanoparticles. The size of the KG-Ag was found to be 19.4 nm. The zeta value for KG, and KG-Ag were found to be  $-28.28 \pm 5.64$ , and  $-4.17 \pm 10.86$  mV, respectively. The polydispersity index (PDI values)

obtained for KG, and KG-AgNPs samples were 0.481 and 0.14 respectively. The PDI values nearing 1 indicate the homogeneity and monodispersity of the polymers (Stepto *et al.*, 2009; Sarwar *et al.*, 2014).

**ICP-MS analysis.** The concentration of silver in KG-AgNPs was found to be 92 ppm by ICP-MS analysis. The individual metal concentrations in KG-AgNPs and ionic metal concentration is depicted in (Table 1). The efficiency of conversion of Ag by Karaya gum was 86%.

**Table 1: Determination of concentration of KG-NPs by ICP-MS and their percent conversion.**

Sr. No.	Sample	Percent (%) metal portion	The concentration of KG-NPs by ICP-MS	Ionic metals Concentrations by ICP-MS	Percent Conversion
1.	Gum karaya	--	--	--	--
2.	AgNPs	--	92 $\mu$ g mL	107 $\mu$ g mL <sup>-1</sup>	86%

**Antibacterial assays of the KG-based silver nanoparticles**

**Well diffusion assay.** The antibacterial activity of the synthesized gum-karaya-based silver nanoparticles (KG-AgNPs) was assessed by the well diffusion method (Kora *et al.*, 2010). The results observed are presented in Fig. 10. depicting the zone of inhibition (ZOI). The ZOI is measured (mm) with KG-AgNPs against both gram-positive and gram-negative strains

are represented in Table 1. The ZOI for *S. aureus* was 13 mm and for *P. aeruginosa* was 15mm at (15  $\mu$ g/mL). Autoclaved gum karaya (1%) used as negative control did not show any zone of inhibition. However antibiotic amikacin used as positive control showed 16 and 18 mm zone of inhibition for *S. aureus* and *P. aeruginosa* respectively. These results revealed that bacterial growth was efficiently inhibited at minimum concentrations of KG-AgNPs.

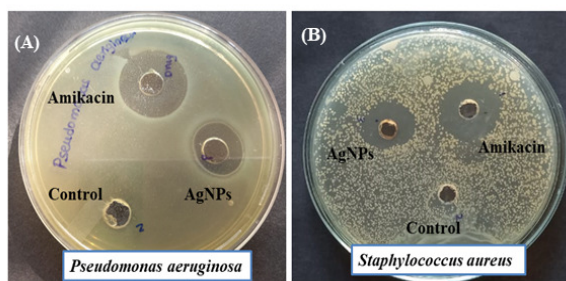


**Fig. 10.** The bacterial culture plates showing the zone of inhibition (mm) around the wells loaded with KG-NPs for Gram-negative (A) (*P. aeruginosa*) and Gram-positive bacterial strains (B) (*S. aureus*).

**Table 2: Determination of ZOI values for synthesized gum karaya-based nanoparticles along with positive (Amikacin) and negative (1% Karaya gum) controls.**

Sample	<i>P. aeruginosa</i> (ZOI)	<i>S. aureus</i> (ZOI)
KG-AgNPs	15mm	13mm
Positive Control (Amikacin)	18mm	16mm
Negative Control (1% Gum Karaya)	0	0

**Micro-broth dilution method.** The minimum inhibitory concentration (MIC) of KG-AgNPs against *S. aureus* and *P. aeruginosa* bacteria was determined. Antibiotic amikacin and Karaya gum 1% were used as positive and negative controls for comparison. The MICs of KG-AgNPs against *P. aeruginosa* and *S. aureus* were 10 and 14  $\mu$ g/mL respectively.

**Mechanism of action of KG-AgNPs**

**Measurement of Cytoplasmic contents from the bacterial cell.** The effect of the NPs on the bacterial membrane was determined by monitoring the cytoplasmic leakage (nucleotides and proteins) as a function of the absorbance (at  $\lambda_{260}$  nm and  $\lambda_{280}$  nm) of the cells treated (Fig. 11). Karaya gum (1%) was used

as negative control and heat-treated bacterial strains were considered as a positive control. An increase in the absorbance of 0.36 at 260 nm and 0.198 at 280 nm was recorded for *S. aureus* respectively when compared with the negative control. Similarly, for *P. aeruginosa* the absorbance values recorded are 0.83 at 260 nm and 0.49 at 280 nm respectively when compared with the negative control indicating leakage. The heat-treated bacterial cells exhibited enhanced cytoplasmic leakage as evidenced by the absorbance of 0.61 at 260 nm and 0.45 at 280 nm recorded for *S. aureus* respectively, whereas in heat-treated *P. aeruginosa* the absorbance values recorded are 0.91 at 260 nm and 0.52 at 280 nm respectively.



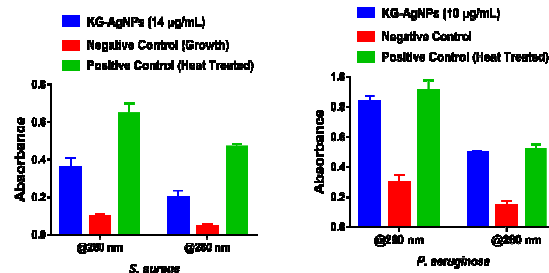


**Fig. 11.** UV-visible absorption at 260nm and 280nm of cytoplasmic contents released from *S. aureus* and *P. aeruginosa* treated with KG-AgNPs, positive (heat treated) and negative controls (not treated) respectively. The values reported are mean  $\pm$  SD.

**Measurement of Intracellular potassium (K<sup>+</sup>) ion leakage.** The leakage of cytoplasmic potassium ions (Tiwari *et al.*, 2008; Kora and Sashidhar 2015) from the bacterial cell membrane of *S. aureus* and *P. aeruginosa* treated with KG-AgNPs was also quantified. The K<sup>+</sup> ion concentration ( $\mu\text{g/mL}$ ) leaked from *S. aureus* and *P. aeruginosa* was found to be 63 and 41  $\mu\text{g/mL}$  respectively when compared with controls (Fig. 12).

**Measurement of intracellular reactive oxygen species (ROS).** Elevated levels of ROS were detected in *S. aureus* and *P. aeruginosa* upon treatment with KG-AgNPs (Kora and Sashidhar 2015; Malkapur *et al.*, 2017). Amongst these *S. aureus* treated with KG-AgNPs displayed enhanced fluorescence when compared with the negative and the positive controls. The study indicated the role of KG-AgNPs in the elevation of ROS and oxidative stress (Fig. 13).

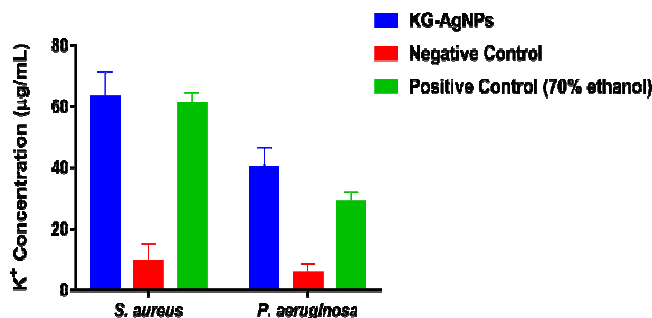


**Fig. 12.** Determination of intracellular K<sup>+</sup> leakage from *S. aureus* and *P. aeruginosa* after treatment with KG-AgNPs. Positive and negative controls were maintained as bacterial cell suspension with 70% ethanol and no drug treatment respectively. The values reported are mean  $\pm$  SD.

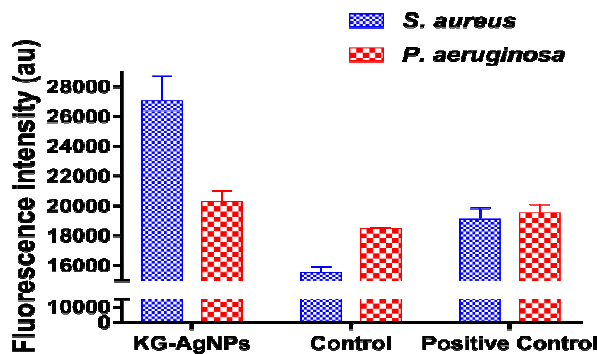


**Fig. 13.** The generation of intracellular reactive oxygen species (ROS) by treating with KG-AgNPs indicated by fluorescence intensity, along with positive (30 $\mu\text{M}$  H<sub>2</sub>O<sub>2</sub>) and negative control (untreated). The values reported are mean  $\pm$  SD.

**Scanning Electron Microscopy Studies.** The cellular damage that occurred in both Gram-positive (*S. aureus*) and Gram-negative (*P. aeruginosa*) bacteria was evaluated by scanning electron microscopy (SEM). The results revealed an intact, smooth surface without any visible cell lysis or debris, in untreated cells which

signifies that the bacterial cells were healthy. The SEM micrographs of treated *P. aeruginosa* and *S. aureus* with KG-NPs clearly showed gross morphological changes in the bacteria. The images recorded depict partial membrane blebbing, budding, the presence of extracellular debris, irregular shapes, and the release of

cellular contents (cell lysis) within 12h of treatment (KG-AgNPs) and were similar to positive control cells that are exposed to a higher temperature. The samples treated with KG-AgNPs also displayed a strong

absorption peak at 3 keV, which further affirms the permeation of silver nanoparticles into the membrane (Fig. 14 and 15).

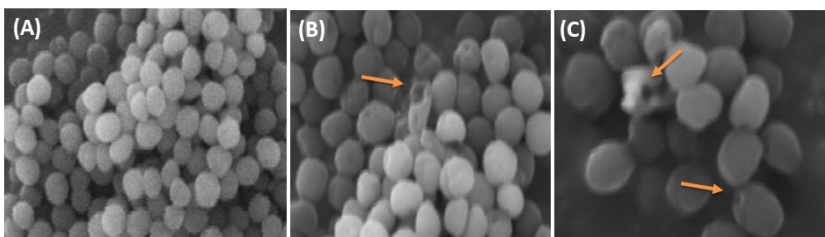


**Fig. 14.** Scanning Electron Microscopy (SEM) images of Gram-positive (*S. aureus*) bacteria. (A) Growth control (B) Heat Control (C) KG-AgNPs treated *S. aureus*. All images are at the scale of 1  $\mu$ m size.

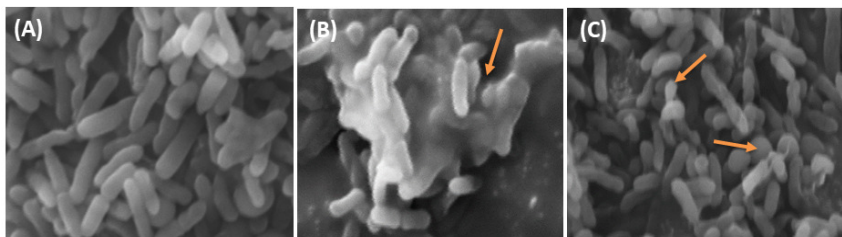


**Fig. 15.** Scanning Electron Microscopy (SEM) images of Gram-negative (*P. aeruginosa*) bacteria. (A) Growth control (B) Heat Control (C) KG-AgNPs treated *P. aeruginosa*. All images are at the scale of 1  $\mu$ m size.

## CONCLUSIONS

The present investigation, reports the synthesis of silver nanoparticles using karaya gum as a stabilizing and reducing agent by the green chemistry approach. The as synthesized KG-AgNPs were successfully characterized by UV-Vis spectroscopic analysis, FT-IR, TEM, SEM, and XRD. The synthesized KG-NPs showed optimal antibacterial activities against *S. aureus* and *P. aeruginosa*. The KG-AgNPs exhibited cytoplasmic leakage studies, membrane damage, disrupted permeability, and enhanced ROS production against both gram-positive and gram-negative bacteria in comparison to amikacin, a standard antibiotic. In conclusion, the results of the current study indicate that the karaya gum-based AgNPs have potential antibacterial activity. The study encourages to further improve in terms of the synthesis of desired nanostructures (size and shape) with extensive applications in the development of potential nano drugs that can target bacteria particularly multidrug-resistant ones, various other microbial pathogens, and also as biosensors in diagnostics.

## FUTURE SCOPE

Karaya gum, a natural, non-toxic, polysaccharide derived from the dried exudate of *Sterculia urens* that acts as a stabilizing and reducing agent, is a suitable biogenic template for synthesizing metal nanocomposites. The mechanistic implications and mode of action of KG-AgNPs investigated were further used to analyze their antibacterial properties. The KG-NPs can be employed as potential therapeutic agents against drug-resistant bacteria. The biocompatible and safe properties also give scope for further investigation of these nanocomposites for the elimination of harmful

microbes in clinical and domestic areas and open new avenues in the field of nanomedicine.

**Acknowledgment.** The authors acknowledge the DST-PURSE-II program (C-DST-PURSE-II/6/17) Government of India New Delhi, at Osmania University for providing the infrastructure facilities.

**Conflict of Interest.** None.

## REFERENCES

- Anderson, D.M.W., and Stoddart, J.F., (1966). Studies on uronic acid materials. *Carbohydr Res*, 2, 104–114.
- Costa, N. J. S. and Rossi, L. M. (2012). Synthesis of supported metal nanoparticle catalysts using ligand-assisted methods. *Nanoscale*, 4(19), 5826–5834.
- Dauthal, P. and Mukhopadhyay, M. (2016). Noble metal nanoparticles: plant-mediated synthesis, mechanistic aspects of Synthesis and applications. *Industrial and Engineering Chemistry Research*, 55(36), 9557–9577.
- Dutta, P., Das, G., Boruah, S., Kumari, A., Mahanta, M., Yasin, A., Sharma, A. and Deb, L (2021). Nanoparticles as Nano- priming Agent for Antifungal and Antibacterial Activity against Plant Pathogens. *Biological Forum – An International Journal*, 13(3), 476–482.
- Gelatti, L. C., Bonamigo, R. R., Becker, A. P. and Azevedo, P. A. (2009). Methicillin-resistant *Staphylococcus aureus*: emerging community dissemination. *A Bras Dermatol Journal*, 84, 501–506.
- Guschin, A. Ryzhikh, P. and Rumyantseva, T. (2015). Treatment efficacy, treatment failures and selection of macrolide resistance in patients with high load of *Mycoplasma genitalium* during treatment of male urethritis with josamycin, *BMC Infectious Disease.*, 15, pp. 1-7.
- Jaiswal, S., Duffy, B. and Jaiswal, A. K. (2010). 'Enhancement of the antibacterial properties of silver nanoparticles using beta-cyclodextrin as a capping agent', *International Journal of Antimicrobial Agents*, 36 (3), 280–283.

- Kalaignana, S., Mahesh Kumar, J. and Sashidhar, R. B. (2017). Anti-proliferative activity of Gum kondagogu (*Cochlospermum gossypium*)-gold nanoparticle constructs on B16F10 melanoma cells: An in vitro model, *Bioactive Carbohydrates and Dietary Fibre*, *V 11*, P 38-47.
- Kora, A. J., Sashidhar, R. B. and Arunachalam, J. (2010). Gum kondagogu (*Cochlospermum gossypium*): A template for the green synthesis and stabilization of silver nanoparticles with antibacterial applications. *Carbohydrate Polymers*, *82*(3), 670-679.
- Kora, A. J., and Sashidhar, R. B., (2015). Antibacterial activity of biogenic silver nanoparticles synthesized with gum ghatti and gum olibanum: A comparative study. *The Journal of Antibiotics*, *68*(2), 88-97.
- Kumari, A., Chetna, Rastogi, V., Someshekar, B. and Christina, E. (2021). Comparative Analysis of effect of Nanoparticles Synthesized by Chemical and Green Methods on Seed Germination: A Review. *Biological Forum-An International Journal*, *13*(2), 237-247.
- Mahapatra, D., Kumar Bharti, S. and Asati, V. (2017). 'Nature inspired green fabrication technology for silver nanoparticles, *Current Nanomedicine*, *7* (1), pp. 5–24.
- Malkapur, D., Devi, M. S., Rupula, K. and Sashidhar, R. B. (2017). Biogenic synthesis, characterization and antifungal activity of gum kondagogu silver nano bio composite construct: assessment of its mode of action. *IET Nanobiotechnology*, *11*(7), 866- 873.
- Martin, I. Sawatzky, P. and Liu, G. (2015). Antimicrobial resistance to *Neisseria gonorrhoeae* in Canada: 2009–2013. *Canada Communicable Disease Report*, *41*, pp. 40-41.
- Mayers, D. L., Lerner, S. A. and Ouelette, M. (2009). Antimicrobial Drug Resistance C: Clinical and Epidemiological Aspects, vol.2, *Springer Dordrecht Heidelberg. Landon*, pp 681-1347.
- Muchintala, D., Suresh, V., Raju, D. and Sashidhar, R. B. (2020). Synthesis and characterization of cecropin peptide-based silver nanocomposites: Its antibacterial activity and mode of action. *Materials Science and Engineering, C*, *110*, 110712.
- Natsuki, J., Natsuki, T. and Hashimoto, Y. (2015). A review of silver nanoparticles: synthesis methods, properties, and applications. *International Journal of Materials Science and Applications*, *4*, 325–332.
- Rai, M., Yadav, A. and Gade, A. (2009). Silver nanoparticles as a new generation of antimicrobials. *Biotechnology Advances*, *27*(1), 76–83.
- Rastogi, L., Kora, A. J. and Sashidhar, R. B. (2015). Antibacterial effects of gum kondagogu reduced/stabilized silver nanoparticles in combination with various antibiotics: a mechanistic approach. *Applied Nanoscience (Switzerland)*, *5*(5), 535-543.
- Sarwar, A., Katas, H. and Zin, N. M. (2014). Antibacterial effects of chitosan– tripolyphosphate nanoparticles: Impact of particlesize molecular weight. *Journal of Nanoparticle Research*, *16*, (7), 2517–2519.
- Seema, M., Manoj, R., Madhuri, S. and Maheshwar, S. (2016). Suitability of Carbon Nanotubes as Drug Carrier. *International Journal of Theoretical & Applied Sciences*, *8*(2), 50-53.
- Srikanth, S., Giri, D. and Pal, D. (2016). Green synthesis of silver nanoparticles: A review. *Green and Sustainable Chemistry*, *6*, pp. 34–56.
- Stepito, R. F. T., Gilbert, R. G., Hess, M., Jenkins, A. D., Jones, R. G. and Kratochvíl, P. (2009). Dispersity in polymer Science, *Pure and Applied Chemistry*, *81*(2), 351–353.
- Subbaiah, K. S. and Beedu, S. R. (2018). Biogenic synthesis of biopolymers-based Ag-Au bimetallic nanoparticle constructs and their anti-proliferative assessment. *IET Nanotechnology*, *12*(8), 1047-1055.
- Tiwari, D. K., Behari, J. and Sem, P. (2008). Time & dose-dependent antimicrobial potential of Ag nanoparticles synthesized by top-down approach. *Current Science*, *95*, 647-655.
- Velpula, S., Beedu, S. R. and Rupula, K. (2022). Biopolymer-based trimetallic nanocomposite synthesis, characterization and its application in the catalytic degradation of 4-nitrophenol. *Journal of Material Science: Materials in Electronics*, *33*, 2677-2698.
- Velpula, S., Beedu, S. R. and and Rupula, K. (2021). Bimetallic nanocomposite (Ag-Au, Ag-Pd, Au-Pd) synthesis using gum kondagogu a natural biopolymer and their catalytic potentials in the degradation of 4-nitrophenol. *International Journal of Biological Macromolecule*; *190*, 159-169.
- Venkatesham, M. Ayodhya, D. and Madhusudhan, A. (2014). A novel green synthesis of silver nanoparticles using gum karaya: Characterization, Antimicrobial activity, and Catalytic activity studies. *Journal of Cluster Science*, *25*, 409-422.
- Vinod, V. T. P. and Sashidhar, R. B. (2011). Bioremediation of industrial toxic metals with gum kondagogu (*Cochlospermum Gossypium*): A natural carbohydrate biopolymer. *In Indian Journal of Biotechnology* (Vol. 10).

**How to cite this article:** Shyamala Chandra Rokkal, Vidya Chernapalli, Suresh Velpula and Karuna Rupula (2023). Autoclave-assisted Green Synthesis of Gumkaraya-based Silver nanoparticles and its Antibacterial Potentials. *Biological Forum – An International Journal*, *15*(3): 181-191.